Quaternary Research 83 (2015) 479–487

Contents lists available at ScienceDirect

Quaternary Research

journal homepage: www.elsevier.com/locate/yqres

Quaternary chronostratigraphy and stable isotope paleoecology of Big Bone Lick, Kentucky, USA

Kenneth Barnett Tankersley [a,b], Madhav Krishna Murari [b,*], Brooke E. Crowley [a,b], Lewis A. Owen [b], Glenn W. Storrs [b,c], Litsa Mortensen [a]

[a] Quaternary and Anthropocene Research Group, Department of Anthropology, University of Cincinnati, Cincinnati, OH 45221, USA
[b] Quaternary and Anthropocene Research Group, Department of Geology, University of Cincinnati, Cincinnati, OH 45221, USA
[c] Cincinnati Museum Center, Cincinnati, OH 45203, USA

ARTICLE INFO

Article history:
Received 4 August 2014
Available online 6 March 2015

Keywords:
Vertebrate fossils
Stable isotopes
Optically stimulated luminescence dating
Radiocarbon dating
Sedimentology

ABSTRACT

Big Bone Lick (BBL) in northern Kentucky, USA has been a critical geologic site in the historical development of North American Quaternary vertebrate paleontology since the 1700s. Sedimentology, geoarcheology, paleontology, accelerator mass spectrometry radiocarbon and optically stimulated luminescence dating, and stable carbon and nitrogen isotope analyses were undertaken to develop a chronostratigraphy and history of erosion and deposition for the site to provide a foundation for understanding taphonomy, and species extinction and adaptation to periods of climatic and environmental change. Three geomorphic surfaces are recognized at BBL representing significant periods of floodplain aggradation since the last glacial maximum (26.5–19 ka) dating to the Oldest Dryas (Tazewell, 25–19 ka), the Older Dryas (Cary, 14–12 ka), and late Holocene (5 ka to the present). Unconformities suggest significant periods of degradation during the transitions from cold and dry to warm and moist climates from the Oldest Dryas (Tazewell) to Bølling Oscillation, from the Older Dryas (Cary) to the Allerød, and from the Younger Dryas (Valders) to the Holocene Climatic Optimum. Increased anthropogenic activities since ~5 ka may have increased soil upland erosion and floodplain aggradation. Stable isotopes demonstrate that the landscape has been dominated by C_3 vegetation since the last glacial maximum.

Introduction

Big Bone Lick (BBL), which is often referred to as the birthplace of American vertebrate paleontology, is in Boone County, Kentucky, approximately 30 km south of Cincinnati, Ohio, USA (Fig. 1, Hedeen, 2008). The history of paleontological discoveries at the site dates back to the early 1700s (Schultz et al., 1963; Levin et al., 1965; Ives et al., 1967; Tankersley, 1990, 1996, 2002; Hedeen, 2008). Yet, despite the historical and paleontological importance of BBL, comprehensive Quaternary research has not been previously conducted at this locality. While the site has been sporadically examined over the last five decades, there has been no systematic research on its chronostratigraphy or stable isotope paleoecology. In order to determine the depositional history and provide a framework for future Quaternary studies at BBL, we examined the Quaternary geology of the terrace and floodplain deposits lining the valley walls of Big Bone Lick Creek and its tributary, Gum Branch, using solid-sediment cores, stream profile paleontological and archeological excavations, radiocarbon (^{14}C) and optically stimulated luminescence (OSL) dating, and stable carbon and nitrogen isotope analyses.

* Corresponding author. Fax: +1 513 556 5784.
E-mail address: murarimk@ucmail.uc.edu (M.K. Murari).

Study area

BBL is located in the glaciated Outer Bluegrass region of Kentucky in a drainage basin that is directly tributary to the glaciated Lower Ohio River Valley (Fig. 2). The site is drained by Big Bone and Gum Branch creeks, which are eroded into Upper Ordovician Cincinnatian Series shales and limestones. The BBL valley was part of the pre-glacial Kentucky River basin (also known as the Cincinnati River), which was a major tributary of the Teays River (Ray, 1974). The BBL valley, which Big Bone Creek and Gum Branch drain, is filled with late Quaternary sediments. Late Cenozoic alluvial gravels from the high-level pre-glacial channel of Eagle Creek, a tributary of the northeast-flowing Kentucky River, cap the hills above the BBL valley in Boone County, Kentucky (Potter, 1996). BBL was located less than 10 km from the margin of the Illinoian ice sheet, and about 50 km from the southern margin of the Laurentide ice sheet during the Wisconsinan glaciation. Oscillations of the margin of the Laurentide ice sheet and consequent hydrological changes resulted in a series of terraces along the BBL valley walls (Fig. 3).

A $CaCl_2$ brine discharges at the surface of Big Bone Creek valley under high hydrostatic pressure through fault planes, joints and bedrock fractures in the Upper Ordovician Cincinnatian rocks (Tankersley, 2007, 2009). The brine originates in a basinal reservoir of Ca-rich and

http://dx.doi.org/10.1016/j.yqres.2015.01.009

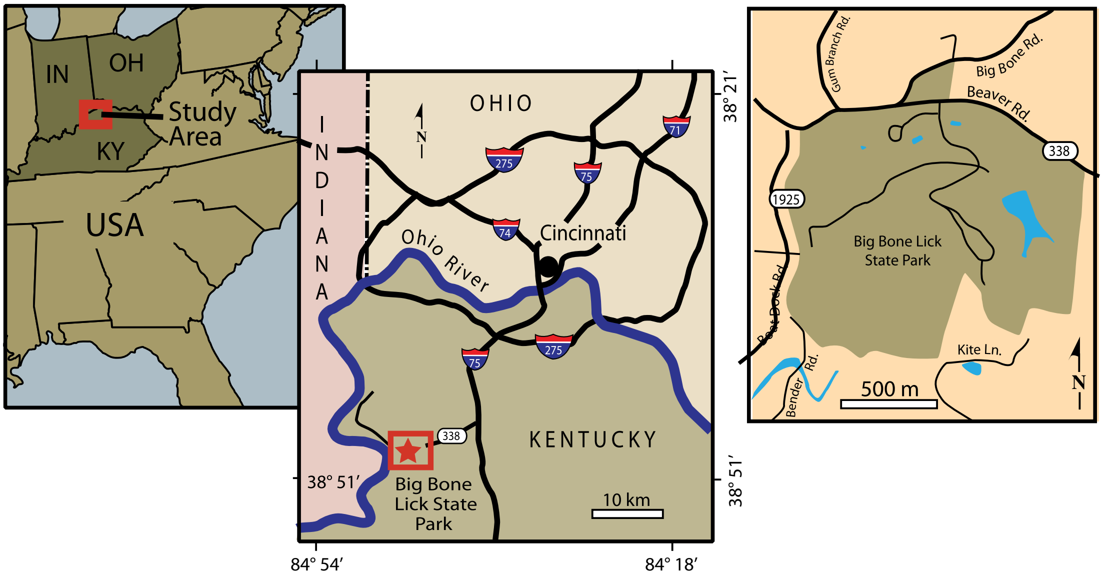

Figure 1. Location of Big Bone Lick State Park.

SO_4-poor paleo-seawater, which sits about 200 m below the present land surface in the permeable Middle Ordovician St. Peter Sandstone Formation (Tankersley et al., 2009). The most prominent brine springs are located near the confluence of Big Bone Creek and Gum Branch. Seasonal creek overbank flooding and Ohio River backwater flooding, plus the recharge of numerous saline springs on the surface of Oldest Dryas (Tazewell) lacustrine deposits (19–25 ka) have continuously maintained a wetland in the valley for thousands of years (Tankersley, 1985). Since the Allerød, saline springs and the surrounding salt licks have attracted a community of large mammals as well as the people who hunted and scavenged these species (Tankersley, 1996; Storrs et al., 2009).

Methods

Field methods

We extracted 18 solid-sediment cores using a JMC Sub-soil Probe. Samples were collected in PETG copolyester liners 1 m in length and 3 cm in diameter (Fig. 4). Additionally, we hand excavated five 2-m

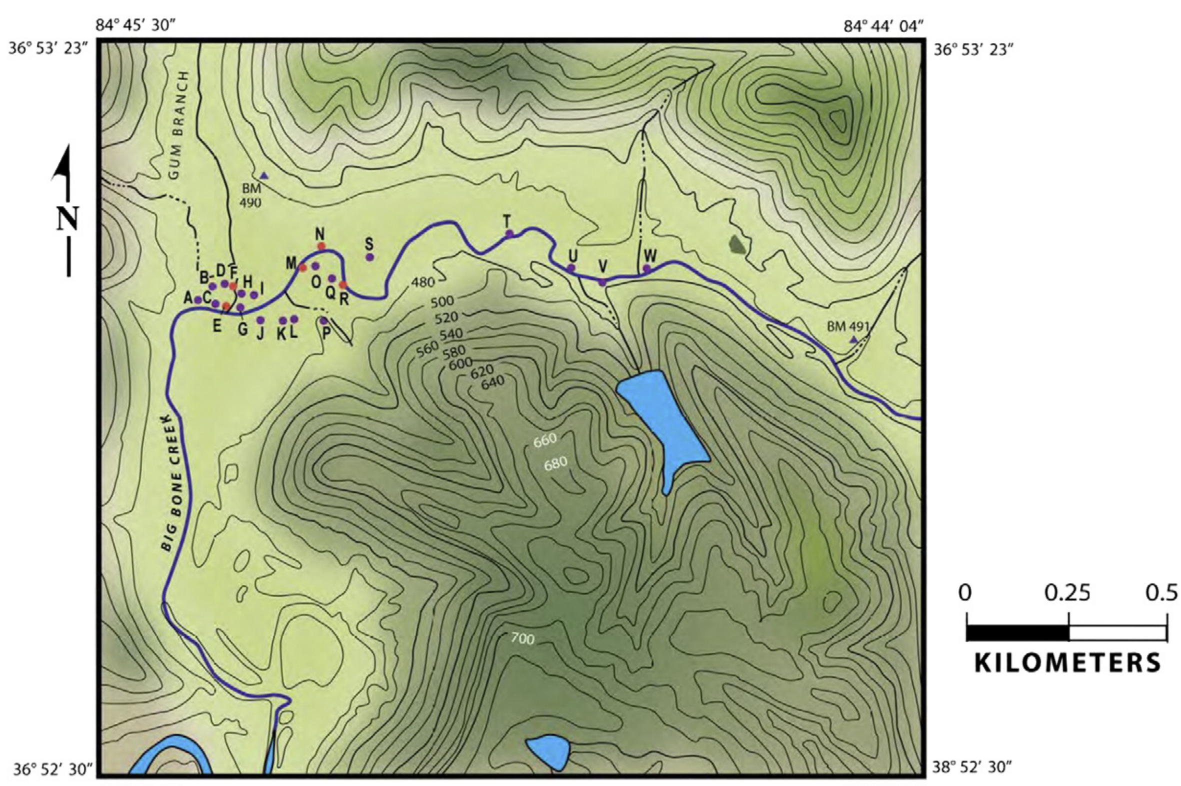

Figure 2. Topographic map of Big Bone Lick showing the locations of solid sediment cores (purple) and profile excavations (red). Elevation is presented in feet above sea level.

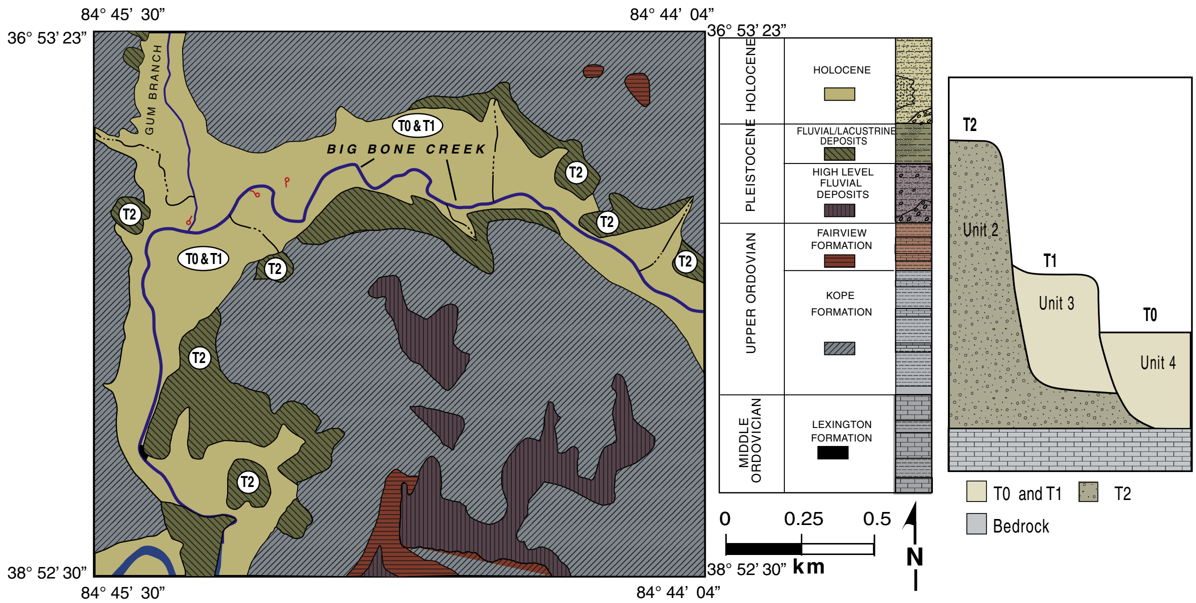

Figure 3. A) Geological map of Big Bone Lick, Kentucky (modified from Tankersley, 1985; Tankersley et al., 2009) covering the same area shown in Fig. 2, and indicating the location of terraces. The small red circles with tails mark the locations of springs. B) Schematic cross-section showing terrace names and units.

wide profile excavations of natural exposures in late Pleistocene terraces (T1 and T2) as well as the Holocene floodplain (T0) of Big Bone and Gum Branch creeks (Figs. 2 and 3). Sediment, plant, and vertebrate remains contained in these profiles were recovered for chronologic dating and stable isotope analyses. Geoarcheological and paleontological profile excavation locations were selected to increase the chronometric resolution of the Quaternary stratigraphy. Interpretations of these profiles were supplemented by prior geoarcheological and paleontological investigations. Excavation profiles were hand dug and all sediments were screened through 0.3 cm screens (Mortensen, 2013). Additional samples were subjected to fine-mesh (<75 μm) water screening to recover small vertebrate, invertebrate, and plant remains for taxonomic identification. Terraces along Big Bone and Gum Branch creeks were mapped based on their morphostratigraphic relationships; younger stream terraces are inset into older stream terraces and occur at lower elevations. The surfaces of these terraces were numbered based on their ages, where T0 is the youngest. The stream terraces are composed of sedimentary units, which were described in natural exposures, profile excavations and sediment cores. Sedimentary units are numbered based on their ages, where Unit 1 is the oldest (see Table 1, Fig. 3). Stratigraphic units were characterized using Munsell soil color, sedimentary structures and particle size analysis.

OSL samples were collected from Holocene floodplain strata in the valleys of Big Bone and Gum Branch creeks. We recorded the depth below the surface, stratum thickness, Munsell soil color, and lithology. Samples were collected by hammering 25 cm-long, 5 cm-diameter

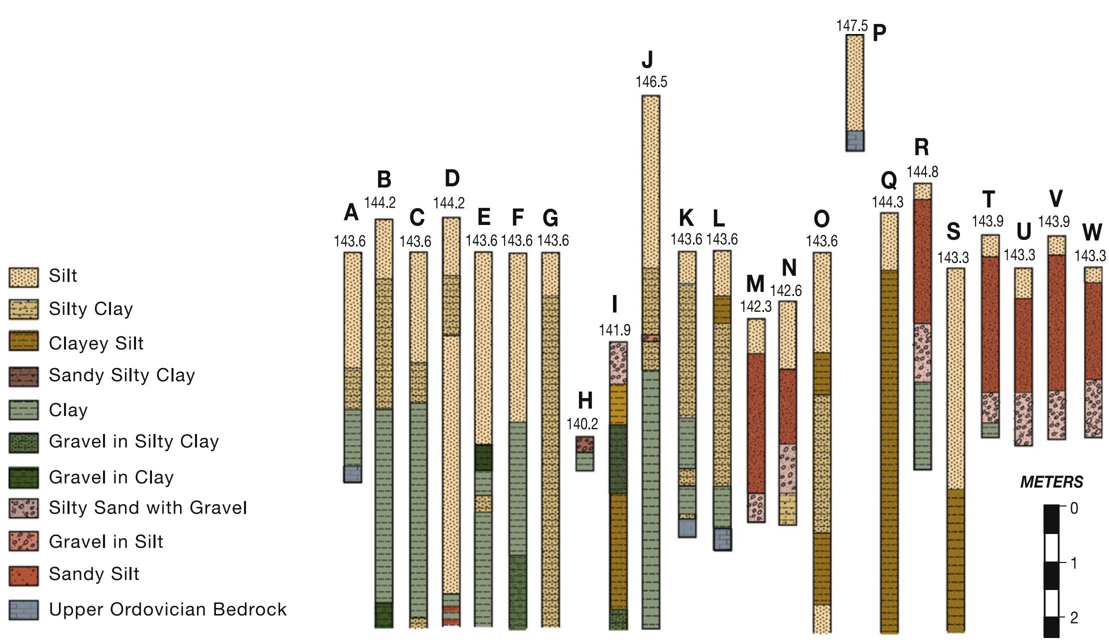

Figure 4. Surficial late Pleistocene and Holocene sediments at Big Bone Lick, Kentucky based on 18 solid sediment cores and 5 profile excavations (E, F, M, N and R, highlighted in red letters). The locations of the cores and excavations are shown in Fig. 2. The numbers above each core refer to the altitude of the surface (meters asl) from which the core was collected.

Table 1
Geomorphic surfaces and stratigraphic units at Big Bone Lick, Kentucky.

Geomorphic surface	Elevation (m)	Unit	Thickness (m)	Age (cal yr BP)	Climatic period
Floodplain (T0)	140–143	4	6	5000–Modern	Holocene
1st terrace (T1)	143–145	3	8	11,630–14,040	Older Dryas
2nd terrace (T2)	147–148	2	10	18,560–25,520	Oldest Dryas
3rd terrace (T3)	>230	1	7	Unknown	Unknown

steel tubes into cleaned, sediment faces. The tubes remained sealed until opened in the Luminescence Dating Laboratory at the University of Cincinnati.

Laboratory methods

Organic remains were hand-selected for radiocarbon dating and stable isotope analysis. Wood samples (20–50 mg) selected for AMS radiocarbon dating were air-dried. All non-wood particles, such as sediment and rootlets, were physically removed using tweezers and a scalpel. The samples were then hand-pulverized to increase the surface area for chemical pretreatment. The pulverized wood was subjected to a standard acid–base–acid pretreatment, washed with hot (85°C) 0.2 M HCl to dissolve carbonates followed by a hot (60°C) 0.2 M NaOH wash to remove organic acids, and a final HCl rinse to neutralize the NaOH. Cellulose was extracted by immersing the sample in temperature controlled (70°C) 0.25 M $NaClO_2$. Beta analytic undertook the radiocarbon dating.

Samples of cortical bone destined for collagen isolation were selected from fragmented but identifiable large mammal bones. Collagen was isolated following the methods outlined in Crowley et al. (2011). Approximately 200 mg of bone was fragmented using a mortar and pestle and then soaked in 0.5 M ethylenediaminetetraacetic acid (EDTA) until demineralized (~25 days). Samples were rinsed using ultrapure Milli-Q water, gelatinized in 0.01 HCl, passed through 1.5 μm glass fiber filters and freeze dried. Tooth enamel samples destined for bioapatite analysis were prepared following Crowley and Wheatley (2014). Approximately 10 mg of enamel was sampled from isolated deciduous mastodon molars using a handheld rotary dremel equipped with a dental bit. Powdered enamel was treated with 30% H_2O_2 for 24 h at room temperature and rinsed with ultrapure water. Samples were then treated with 1 M Ca-buffered acetic acid for 24 h at 4°C, rinsed, and freeze-dried. Collagen was analyzed at the University of California, Santa Cruz using a Carlo Erba 1108 elemental analyzer interfaced to a Thermo Finnigan Delta Plus XP isotope ratio mass spectrometer. Data were corrected using IAEA Acetanilide and an internal gelatin standard. Enamel carbonate was analyzed at the Illinois State Geological Survey, Prairie Research Institute. Samples were run on a Kiel III automated carbonate preparation device coupled to a Finnigan MAT 252 isotope ratio mass spectrometer. Samples were reacted with orthophosphoric acid at 70°C for 10 min. Carbon and nitrogen isotope data are reported relative to international standards Vienna Pee Dee Belemnite (VPDB) and atmospheric nitrogen (AIR). Data were corrected using NBS-18 and NBS-19. Radiocarbon ages obtained from bone collagen were run at the Center for Accelerator Mass Spectrometry, Lawrence Livermore National Laboratory.

Sediment samples (10 cm^3) destined for bulk stable carbon isotope analysis were air-dried and hand reduced to a powder (<75 μm) using a mortar and pestle. Bulk organic matter was decalcified at room temperature in a 1 N HCl bath overnight (i.e., >12 h). The acid was rinsed out of each sample with distilled, deionized, demineralized water until the pH was neutral. While an hour-long 1 N HCl bath at room temperature is usually adequate to remove carbonates from sediment samples, extended acidification was necessary to remove all mineral calcite and prevent an artificial enrichment of the $\delta^{13}C$ values in the bulk organic samples. Stable carbon isotopes were analyzed at the Center for Applied Isotope Studies at the University of Georgia using a Finnigan MAT 252 Isotope Ratio Mass Spectrometer.

Sediments destined for OSL dating were removed from the end of the sample tubes and dried to determine the water content. This sediment was then crushed and sent to Activation Laboratories Limited in Ancaster, Ontario, Canada for Major Elements Fusion ICP/MS/Trace Elements analysis to determine the U, Th and K concentrations for dose rate (D_R) calculations (Table 2).

Sediment from the center of the tubes and cores was pretreated with 10% HCl and 10% H_2O_2 to remove carbonates and organic matter, respectively. The pretreated samples were rinsed in water, dried and sieved to attract the 90–150 μm particle size fraction. A low field controlled Frantz isodynamic magnetic separator (LFC Model-2) was used to separate feldspar and magnetic minerals from quartz in the 90–150 μm particle size fraction following the methods of Porart (2006) with the forward and side slopes set at 100° and 10°, respectively, within a variable magnetic field. The quartz-rich separate was etched using 44% HF for 80 min to remove the outer alpha irradiated layer from quartz particles and any feldspars that were removed during the magnetic separation.

Any fluoride precipitates were removed using concentrated HCl. The quartz sample was then rinsed in distilled water and acetate, and dried and sieved to obtain the 90-150 μm grain size fraction. An automated Risø OSL reader model TL-DA-20 was used for OSL measurements and irradiation. Aliquots, containing approximately 100 grains of the samples, were mounted onto ~6 mm-diameter stainless steel disks as a small central circle ~ 2 mm in diameter. Aliquots for each sample were first checked for feldspar contamination using infrared stimulated luminescence (IRSL) at room temperature before the main OSL measurements were undertaken (after Jain and Singhvi, 2001). If the aliquots did not pass the IRSL test the samples were etched in 40% HF for an additional 30 min to remove any feldspar, followed by 10% HCl treatment and sieving again. Ultimately, samples that passed IRSL test were used for OSL dating.

Aliquots of samples were illuminated with blue LEDs stimulating at a wavelength of 470 nm (blue light stimulated luminescence — BLSL). The detection optics comprised Hoya U-340 and Schott BG-39 color glass filters coupled to an EMI 9235 QA photomultiplier tube. The samples were irradiated using a $^{90}Sr/^{90}Y$ beta source. The single aliquot regeneration (SAR) method (Murray and Wintle, 2000, 2003) was used to determine the equivalent dose (D_E) for age estimation. Only aliquots that satisfy the criterion of a recycling ratio not more than 10% were used in determining D_E. A preheat of 240°C for 10 s was used and the OSL signal was recorded for 40 s at 125°C. OSL sensitivity of the samples had a high signal to noise ratio.

Descriptions of geomorphic surfaces and allostratigraphic units

The geomorphology and allostratigraphy of BBL have been variously described for more than 150 years (Schultz et al., 1963). Tankersley (2009) and Tankersley et al. (2009) recently identified four distinctive geomorphic surfaces/terraces, including a pre-glacial alluvial terrace, two late Pleistocene terraces (T1 and T2), and a Holocene floodplain (TO), and four major sedimentary units (Figs. 2 and 3, Table 1). The oldest surface is a Teays-age (>400 ka) high-level alluvial deposit at an elevation of ~230 m (700 ft) above sea level (asl). T2 is an Oldest Dryas (Tazewell) terrace at an elevation of ~146 m (480 ft) asl and T1 is an Older Dryas (Cary) terrace at an elevation of ~144 m (473 ft) asl. The Holocene floodplain (T0) sits adjacent to the terraces at an elevation of ~143 m (470 ft) asl. Paleochannels and channel fragments of varying scales with a stratigraphic sequence similar to those present in the neighboring drainage basin tributaries to the glaciated Ohio River Valley are evident (Schultz et al., 1963; Ray, 1974; Gray, 1984).

Unit 1 is a pre-glacial alluvium and the oldest stratigraphically. This unit is a late Tertiary pre-glacial alluvial deposit that forms ridge-tops at elevations > 230 m asl (Potter, 1996) (Fig. 3). The unit is ~7 m thick and composed of deeply weathered, yellowish-brown clayey silt and sand

Table 2
Dose rate estimation for OSL samples.

Sample	U (ppm)	Th (ppm)	K (%)	Water content (%)	Cosmic dose rate (μGy/ka)	Total dose rate (Gy/ka)
BBL1	3.30 ± 0.33	11.2 ± 1.12	2.88 ± 0.14	10.5 ± 2.1	98.62 ± 20	3.90 ± 0.23
BBL2	3.30 ± 0.33	12.3 ± 1.23	2.95 ± 0.15	9.7 ± 1.9	98.62 ± 20	3.29 ± 0.15
BBL3	2.50 ± 0.25	8.5 ± 0.85	2.48 ± 0.12	5.8 ± 1.2	115.00 ± 23	2.81 ± 0.13
BBL7	2.20 ± 0.22	7.5 ± 0.75	2.19 ± 0.11	3.7 ± 0.7	115.00 ± 23	3.46 ± 0.16

with abundant rounded to subangular pebbles and cobbles of chert, quartz, and limonitic concretions.

Unit 2 is an Oldest Dryas (Tazewell) lacustrine deposit that forms T2, the highest and oldest terrace at ~147–148 m asl (Fig. 3). The deposit is ~10 m thick, and composed of a distinctive light gray to brownish-gray stiff clay, clayey silt, gravel in clay, and silty clay with plant and animal remains present (Tankersley et al., 2009).

Unit 3 is a silt-dominated alluvium that dates to the Older Dryas (Cary). The deposit is ~8 m thick and extends about 5 m below the lowest T1 Oldest Dryas (Tazewell) terrace at ~143–145 m asl and 3–5 m above T0, the Holocene floodplain (Fig. 3). In some areas, it is capped with a veneer of Holocene alluvium up to 6 m in thickness. Unit 3 is composed of a weathered yellowish-gray to brown gravelly clay, gravelly silt, gravelly silty clay, and silty clay (Tankersley et al., 2009). Stringers of Upper Ordovician limestone and siltstone pebbles, yellowish orange calcareous concretions, reddish brown limonitic concretions, and plant and animal remains are present.

Unit 4 is a silt-dominated late Holocene alluvial deposit that is ~6 m thick and contains abundant plant and animal remains (Tankersley, 1987; Tankersley et al., 1983). Silt extends downward from the T0 surface, ~140–143 m asl. Upper Ordovician limestone and siltstone pebbles, cobbles, and slabs, as well as well-rounded igneous and metamorphic rock clasts are present.

Dating and stable isotope results

^{14}C dating

We obtained new AMS radiocarbon ages for three wood samples and three bones. Radiocarbon ages were calibrated at 2-sigma to calendar years before present (BP) using the IntCal13 calibration curve in CALIB 7.0 (Reimer et al., 2013). A comprehensive list of new and previously published radiocarbon ages for BBL is provided in Supplementary Table 1. These include: seven conventional β-decay dates (Modern to 4820 cal yr BP), which overlap with seven AMS dates (Modern to 4830 cal yr BP) from Unit 4; one conventional β-decay date (11,630–13,030 cal yr BP), which overlaps with three AMS dates (12,750 to 14,040 cal yr BP) from Unit 3; and one conventional β-decay date (19,380 to 22,290 cal yr BP), which overlaps with two AMS dates (18,560 to 25,520 cal yr BP) from Unit 2.

OSL dating

We were able to obtain ages for all samples that were collected for OSL dating. OSL ages obtained from the late Holocene alluvial deposit (Unit 4) range from ~0.4 ka to ~5.2 ka (Tables 2 and 3). Dose recovery tests (Wintle and Murray, 2006) for each sample show that laboratory doses were recovered within 2% uncertainty by the SAR protocol, suggesting that the protocol was appropriate and add confidence to the dating (Fig. 5). Every aliquot of sample was tested for feldspar contamination using IRSL for a given dose before making real measurement for age estimation. Figure 6 shows the blue light stimulated luminescence (BLSL) and infrared stimulated luminescence (IRSL) for an equivalent dose of 6 Gy. The absence of IRSL confirms the lack of feldspar in the prepared sample. The rapid decay exhibited in shine down curves under BLSL confirms that the OSL signal is dominated by the fast component and hence substantiates the view that partial bleaching is not a problem for these samples.

Stable isotope values

Stable carbon isotope values were obtained for enamel carbonate from two deciduous late Pleistocene mastodon molars and δ^{13}C values and δ^{15}N ratios were obtained for bone collagen from one late Pleistocene proboscidean rib, as well as a rib and scapula from two late Holocene bison (Supplementary Table 2). We also obtained δ^{13}C values for 31 bulk organic matter samples from alluvial and lacustrine strata that range in age from the last glacial maximum to modern (Supplementary Table 3). All faunal remains and sediments were collected from radiocarbon- and OSL-dated sediments exposed in the 2 m-wide stream profile excavations.

Combining these new data with previously published data, we find relatively consistent δ^{13}C and δ^{15}N values among vertebrate taxa excavated from the site (Supplementary Table 2). Carbon isotope values obtained from bone collagen from late Pleistocene proboscideans range from -20.8‰ to -21.9‰ and δ^{15}N values range from 7.5‰ to 6.3‰. Carbon isotope values from late Holocene *Bison bison* bone collagen range from -23.8‰ to -24.1‰ and δ^{15}N isotope ratios ranged from 5.7‰ to 4.4‰. Carbon isotope values for proboscidean and bison enamel carbonate range from -12.9‰ to 13.3‰ and -13.2‰ to -15.4‰, respectively (Supplementary Table 2).

The δ^{13}C values of bulk organic matter were used to determine how the vegetation composition of BBL varied through time. The average δ^{13}C isotope value of bulk organic matter from late Pleistocene sediments ($N = 4$) was -27.1 ± 0.5‰. The average δ^{13}C values of bulk organic matter from late Holocene sediments ($N = 25$) were -26.4 ± 1.1‰.

Discussion

Given the range of uncertainties of the dating methods we used (Table 1 and Supplementary Table 1), the OSL ages (Tables 2 and 3) are remarkably similar to those obtained via conventional β-decay counting and AMS ^{14}C dating. The conventional β-decay dates appear

Table 3
Equivalent dose and dates estimated using single aliquot regenerative (SAR) method. Each date was estimated feeding data in software written by Grun (2009).

Sample	Number of disks[a]	Weighted mean (Gy)	Mean (Gy)	Dose rate (Gy/ka)	Weighted mean age (ka)	Mean age (ka)
BBL1	23 (24)	20.05 ± .01	20.51 ± 2.38	3.90 ± 0.23	5.1 ± 0.1	5.3 ± 0.6
BBL2	22 (24)	21.02 ± 0.01	21.47 ± 2.33	3.29 ± 0.15	5.2 ± 0.1	5.3 ± 0.6
BBL3	22 (24)	1.59 ± 0.001	1.91 ± 0.71	2.81 ± 0.13	0.4 ± 0.01	0.6 ± 0.2
BBL7	21 (24)	3.27 ± 0.002	3.61 ± 1.39	3.46 ± 0.16	0.9 ± 0.02	1.1 ± 0.4

[a] The total number of aliquots measured are listed inside the parentheses while the number of aliquots that were considered for age estimation are listed outside the parentheses.

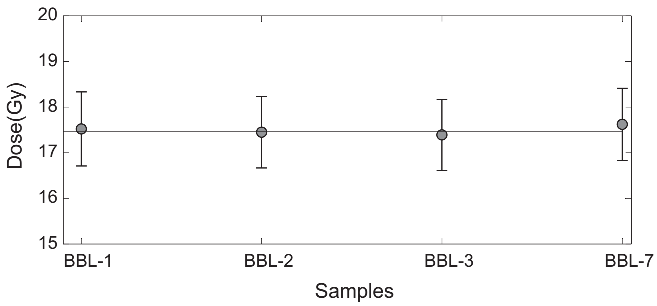

Figure 5. Dose recovery for all BBL samples. A 17.5 Gy dose was recovered for each sample using single aliquot regenerative (SAR) protocol. Error bar shows standard deviation of 5 aliquots.

to be robust based on their comparison with the AMS ^{14}C dates from the same units. For example, the oldest sediments from late Holocene Unit 4 were dated with a conventional β-decay radiocarbon age of 4820–4440 cal yr BP, an AMS radiocarbon age of 4830–4580 cal yr BP, and two OSL ages of 5.2 ± 0.1 ka and 5.1 ± 0.1 ka. Similarly, the most recent sediments from Unit 4 were dated with an AMS radiocarbon age of 480–300 cal yr BP and an OSL age of 0.4 ± 0.01 ka. This corroboration provides evidence that these methods were effective in dating the Quaternary stratigraphic units and landforms at BBL.

Our profile excavations and solid sediment cores indicate that Unit 2 is widespread across the BBL valley and overlain by Unit 3 in T1 and Unit 4 in T0 (Fig. 7). Unit 2, a late Pleistocene lacustrine valley fill, includes heavily mineralized, discolored (black to gray), disarticulated, and fragmented to complete bones and teeth of *Bison bison antiquus* (Ancient Bison), *Bootherium bombifrons* (Woodland Musk Ox), *Cervalces scotti* (Stag Moose), *Equus complicatus* (Complex-Toothed Horse), *Mammut americanum* (American Mastodon), *Mammuthus* sp. (Mammoth), and *Rangifer tarandus* (Caribou) (Supplementary Table 4).

Radiocarbon ages obtained from Unit 2 range from 19,380 to 25,520 cal yr BP. During this time, the greatest volume of meltwater and outwash from the Laurentide ice sheet was channeled into the Ohio River (Ray, 1974). Aggradation of the Ohio River from glacial alluvial outwash and the formation of a valley train dammed the mouths of tributary valleys. As this Oldest Dryas (Tazewell) outwash grew thicker, the depth of ponding in the tributaries increased until the valley train reached its maximum level. Backwaters in the ponded tributaries formed widespread shallow lakes extending more than 20 km from the main valley (Ray, 1974; Potter, 1996; Tankersley, 2007, 2009). River degradation at the time of maximum ice recession resulted in a prominent Oldest Dryas (Tazewell) terrace.

Stable carbon isotope (δ^{13}C) values from bulk organic matter from Unit 2 range from -26.5‰ to -27.6‰, indicating an environment dominated by C_3 vegetation such as spruce (Nadelhoffer and Fry, 1988). Carbon isotope values from proboscidean bone collagen and *Mammut americanum* enamel from Unit 2 are also consistent with a C_3- dominated diet, possibly consisting of coniferous twigs and herbaceous vegetation (Supplementary Table 2) (Vogel et al., 1990; Cerling and Harris, 1999; Metcalfe et al., 2011, 2013), suggesting that BBL was covered by C_3 vegetation during the last glacial maximum.

Unit 3 represents vertical and lateral accretion of alluvial sediments deposited in lithologically similar but temporally distinct strata. Disarticulated yet complete bones of *Mammut americanum* occur in Unit 3 along with heavily mineralized broken and abraded large mammal bones (Supplementary Table 4) (Tankersley, 2009; Tankersley et al., 2009). Radiocarbon ages range from 14,230 to 11,630 cal yr BP. Degradation of the Ohio River continued after the LGM. An ensuing re-advancement resulted in a prominent T1 Older Dryas (Cary) terrace.

Early Paleoindian artifacts such as Clovis spear points, spurred end scrapers, flake knives, and mastodon bones with cut marks also occur in Unit 3 (Tankersley, 2009; Tankersley et al., 2009; Krasinski, 2010). The youngest radiocarbon age from Unit 3 (13.000 to 12.750 cal yr BP) overlaps with the established age range of the Allerød and Clovis technological complex (Tankersley, 1985, 2007, 2009; Tankersley et al., 2009). While the co-occurrence of Clovis artifacts and mastodon bone with human mediated cut-marks in Unit 3 suggests direct human involvement with this species and perhaps others, the contexts are secondary. Like the proboscideans from Unit 2, δ^{13}C and δ^{15}N values obtained from *Mammut americanum* bone collagen from Unit 3 are consistent with mastodons browsing on a wide range of resources in a mosaic environment dominated by C_3 vegetation (Vogel et al., 1990).

Unit 4 consists of a silty sandy alluvium with gravel beds, abundant wood charcoal, freshwater invertebrates (mussels and snails), the remains of C_3 plants and large mammals, and weathered and stream-worn large mammal bones that are likely from Units 2 and 3. Plant species include *Acer saccharinum* (Silver Maple), *Carya* sp. (Hickory), *Juglans cinerea* (Butternut), *Juglans nigra* (Black Walnut), and *Juniperus virginiana* (Red Cedar), and large mammal remains include *Bison bison* (Modern Bison), *Cervus canadensis* (Elk), *Odocoileus virginianus* (White-tailed Deer), and *Ursus americanus* (Black Bear) (Supplementary

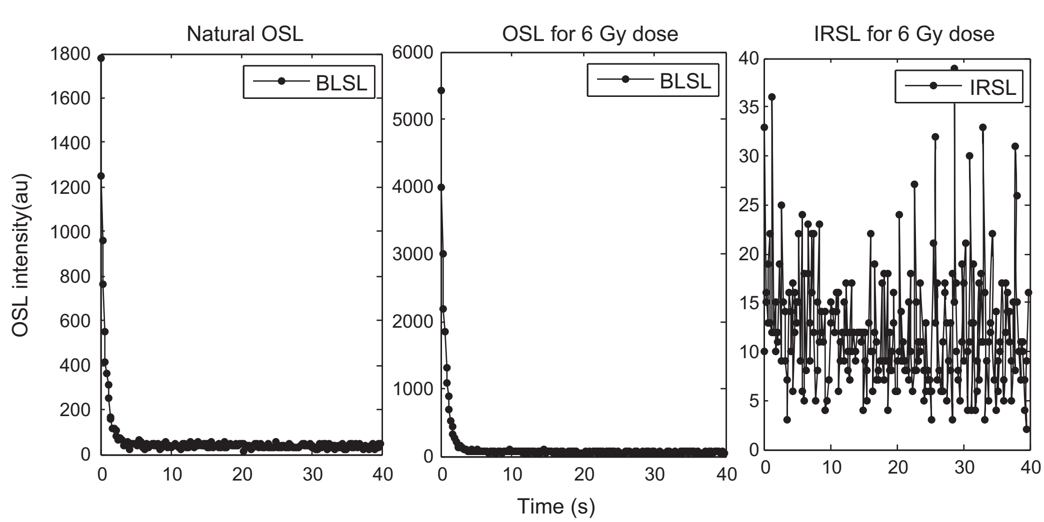

Figure 6. Typical shine down curves for OSL sample BBL3. From the left to right figure shows natural BLSL, OSL for 6 Gy beta dose BLSL, and infrared stimulated luminescence (IRSL) for 6 Gy dose, which confirms the absence of any feldspar in the sample.

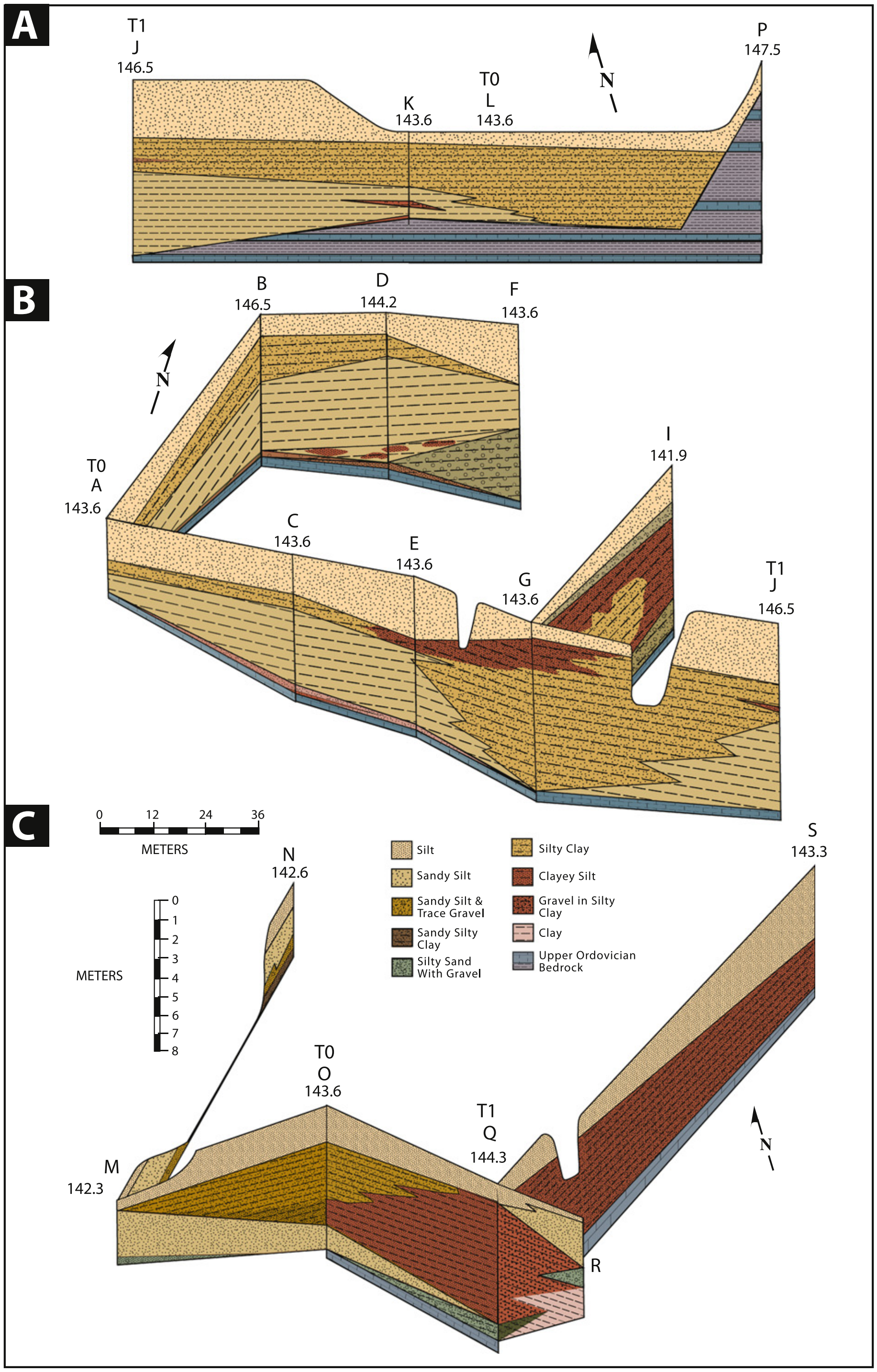

Figure 7. Detailed stratigraphy and sedimentology for the post-Older Dryas (Cary) terrace (T1), and late Holocene floodplain (TO) at Big Bone Lick. Elevation for each core is presented in m asl. Geographic location for the cores is shown in Fig. 2. A) Cross-section of surficial late Pleistocene and Holocene sediments based on exploratory excavation units and cores. B) Fence diagram for the surficial late Pleistocene and Holocene sediments based on exploratory excavation units (A–G, I and J). C) Fence diagram based on exploratory excavation units and cores (M through S).

Table 4). Late Archaic (ca. 2500–5500 cal yr BP), early to late Woodland (ca. 1100–2500 cal yr BP), and early to late Fort Ancient (ca. 300–1100 cal yr BP) artifacts and features occur in stratigraphic succession in Unit 4. Radiocarbon ages for this layer range from Modern to 4830 cal yr BP, and OSL ages range from 0.4 ± 0.01 ka to 5.2 ± 0.1 ka, which are consistent with the artifact typology. Partially articulated and disarticulated bison bones, flaked-stone spear points and arrowheads, flake knives, scrapers, shell tempered late Fort Ancient, Madisonville cord-marked pottery, including salt pans, and musket balls are also present in a layer of Unit 4 just below the present water table. These artifacts are directly associated with late Fort Ancient and Historic Shawnee bison kill and butchering activities during the Little Ice Age, between AD 1550 and 1800 when the last bison was killed at BBL (Tankersley, 1986; Storrs et al., 2009). Most of the $\delta^{13}C$ values from bulk organic matter from Unit 4 range from -25.0‰ to -28.0‰, suggesting an environment dominated by C_3 vegetation. Similar to the late Pleistocene vertebrates, $\delta^{13}C$ and $\delta^{15}N$ values obtained from bison collagen from Unit 4 are consistent with bison browsing on C_3 plants

(Supplementary Table 2). Previously published enamel $\delta^{13}C$ values also indicate that bison had a C_3-based diet at BBL (Widga, 2006; Supplementary Table 2).

The $\delta^{13}C$ and $\delta^{15}N$ values obtained for collagen from Little Ice Age *Bison bison* are slightly lower than those obtained for bone collagen from late Pleistocene proboscideans (Supplementary Table 2). These data suggest that a more open, mosaic environment may have existed during the late Pleistocene compared to the late Holocene, which is in agreement with regional vegetation reconstructions based on pollen (Heusser et al., 2002; Gill et al., 2012; Liu et al., 2013). Conditions were also possibly more arid during the late Pleistocene. Consistent with this scenario, higher $\delta^{13}C$ values combined with slightly elevated $\delta^{15}N$ values in proboscideans suggest that plants might have been more water stressed during the Pleistocene (Handley et al., 1999; Heaton, 1999).

The stable isotope record from BBL seems to be fairly complacent for the late Pleistocene and Holocene. Unfortunately, paleoenvironmental reconstructions based on well-dated pollen profiles for this region are sparse and coarse-grained. While fine-grained pollen data have been obtained for regions north and south of the central Ohio River, there are none available for the area around BBL. However, a large suite of well-dated botanical remains has been recovered from archeological sites in the region that span the late Pleistocene and Holocene (Fig. 8) (Dalbey, 1992; Drooker, 1997). These data show that C_3 plants dominated throughout this time with the exception of a few C_4 plants such as Nimblewill (*Muhlenbergia schreberi*), certain grasses (*Poaceae* family), some species of pigweed (*Amaranthus* sp.), and domesticated corn (*Zea mays*). Additionally, Indian Chickweed (*Mollugo* sp.) is a C3-C4 intermediate. The Panicum genus has C3, C4, and intermediate representatives. Purslane (Portulaca sp.) can shift from a C4 to a CAM photosynthetic pathway. If we assume that each plant taxon had an individualistic response to climatic change, then there would have been an ever-changing complex mosaic of vegetation patches at BBL and the region in the late Pleistocene and Holocene (Fig. 8).

Although allostratigraphic Unit 3 and Unit 4 are discrete entities, in many areas, the texture of the two units is indistinguishable and paleosols are absent. Presently, late Pleistocene floodplain formation cannot be visually distinguished from more recent Holocene events (Ray, 1974). Because there are no visible vertical or horizontal separations between Units 3 and 4, previous investigators have combined them into a single unit (e.g., Swadley, 1969; Ray, 1974). The alluvial surface of Unit 4 was created by lateral accretion of channel deposits and by overbank deposition during late Holocene flooding. Because of the narrow bedrock valley, shifting of Big Bone Lick Creek and Gum Branch has been inhibited, so Unit 4 and its associated terrace (T0) are restricted in areal extent (Ray, 1974).

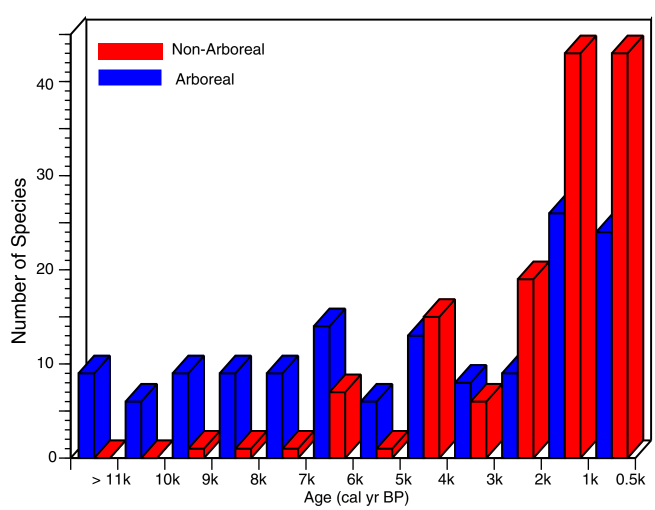

Figure 8. Plant species richness at millennium intervals for different ecological sets (arboreal versus non-arboreal taxa) based on macro-botanical remains from archeological sites in the central Ohio River valley.

There is a ~5000-year allostratigraphic unconformity between Unit 2 and Unit 3, which spans 14–19 ka, from the Oldest Dryas (Tazewell) to the Bølling Oscillation, and a second ~7000-year allostratigraphic unconformity between Unit 3 and Unit 4, spanning 5–12 ka from the Younger Dryas (Valders) to the Holocene Climatic Optimum. These unconformities are chronometrically associated with intensive periods of floodplain degradation and the transition from cool and dry to warm and moist climates. The most intensive interval of Holocene floodplain aggradation (≥4 m) occurred during the late Holocene between ~300 and 5000 cal yr BP.

During this time there is a dramatic increase in the number and size of archeological sites and features on inceptisols in Unit 4. Abundant wood charcoal throughout Unit 4 is likely the result of upland deforestation. Basin-shaped features filled with fire-cracked rocks, wood charcoal, and hickory and walnut shells resulting from the processing of upland masts are also abundant in Unit 4. A dramatic increase in archeological site size and abundance, wood charcoal, and features is associated with a dramatic increase in human population, a trend toward more sedentary livelihood, and landscape modification related to silvaculture, horticulture, and agriculture (Lewis, 1996). These anthropogenic processes could have dramatically increased erosion and accelerated floodplain aggradation and adversely impacted the paleontological record.

Conclusions

Recent AMS radiocarbon dating extends the ages of the bone-bearing deposits of BBL back to the last glacial maximum. Three distinctive geomorphic surfaces and three stratigraphic units date to 19,000–25,000 cal yr BP (T2, Unit 2), 12,000–14,000 cal yr BP (T3, Unit 3), and present to 5000 cal yr BP (T4, Unit 4). Stable isotope data obtained from bulk organic matter indicate that both late Pleistocene (spruce-dominated vegetation) and late Holocene habitats (temperate hardwoods) were dominated by C_3 vegetation. Stable isotope data obtained from bone collagen and enamel also indicates that the landscape was dominated by C_3 vegetation from the last glacial maximum to the present with more open mosaics or drier conditions possibly occurring during the late Pleistocene.

Significant periods of degradation (i.e., channel incision) occurred during the transitions from the cold and dry Oldest Dryas (Tazewell), Older Dryas (Cary), and Younger Dryas (Valders) to the warm and moist Bølling Oscillation, Allerød, and Holocene Climatic Optimum. By 5 ka, anthropogenic landscape modification most likely associated with upland food production (i.e., silvaculture and horticulture) may have resulted in a substantial increase in erosion and floodplain aggradation. These anthropogenic processes predate European colonization of the area by more than 4500 years. Understanding both natural and anthropogenic erosional processes during the Holocene is crucial to our interpretations of the late Pleistocene paleontological record of BBL and other archeological and paleontological sites located in alluvial contexts. There is an inherent danger of oversimplifying these processes, which results in an underlying assumption of landscape change or stability where it does not exist. Furthermore, both natural and anthropogenic erosional processes are directly responsible for the primary and secondary deposition of vertebrate, invertebrate, and plant remains, and artifacts. We hope that paleontologists and archeologists will benefit from the chronostratigraphic framework that we present in this study.

Acknowledgements

The Kentucky State Parks, the Kentucky Office of State Archeology, and Big Bone Lick State Park provided permits for this work. This study was made possible with funding from the Court Family Foundation, the Charles Phelps Taft Foundation, the Cincinnati Museum Center, and the University of Cincinnati Research Council. We would also like to thank Dyke Andreasen, Denis Conover, Shari Fanta, Tom Guilderson, Jeff Speakmann, Todd Young, and Paula Zermeño, for technical assistance, and the students from the 2012, 2013, and 2014 University of Cincinnati Summer Archaeological Field Schools for their contributions to the fieldwork. Thanks to Tim Phillips for drafting most of the figures.

Appendix A. Supplementary data

Supplementary data to this article can be found online at http://dx.doi.org/10.1016/j.yqres.2015.01.009.

References

Cerling, T.E., Harris, J.M., 1999. Carbon isotope fractionation between diet and bioapatite in ungulate mammals and implications for ecological and paleoecological studies. Oecologia 120, 347–363.

Crowley, B.E., Wheatley, P.V., 2014. To bleach or not to bleach: assessing carbon and oxygen isotope variation among apatite preparation techniques. Chemical Geology 381, 234–242.

Crowley, B.E., Godfrey, L.R., Irwin, M.T., 2011. A glance to the past: subfossils, stable isotopes, seed dispersal, and lemur species loss in Southern Madagascar. American Journal of Primatology 73, 25–37.

Dalbey, T.S., 1992. Geological Aspects of Key Archaeological Sites in Northern Kentucky and Southern Ohio. Department of Geological Survey, Columbus.

Drooker, P.B., 1997. The View from Madisonville: Protohistoric Western Fort Ancient Interaction Patterns. Museum of Anthropology Memoirs, No. 31. University of Michigan, Ann Arbor.

Gill, J.L., Williams, J.W., Jackson, S.T., Donnelly, J.P., Schellinger, G.C., 2012. Climatic and megaherbivory controls on late-glacial vegetation dynamics: a new, high-resolution, multi-proxy record from Silver Lake, Ohio. Quaternary Science Reviews 34, 66–80.

Gray, H.H., 1984. Archaeological sedimentology of overbank silt deposition on the floodplain of the Ohio River near Louisville, Kentucky. Journal of Archaeological Sciences 11, 421–432.

Grun, R., 2009. The "AGE" program for the calculation of luminescence age estimates. Ancient TL 27, 45–46.

Handley, L.L., Austin, A.T., Robinson, D., Scrimgeour, C.M., Raven, J.A., Heaton, T.H.E., Schmidt, S., Stewart, G.R., 1999. The ^{15}N natural abundance of $\delta^{15}N$ of ecosystem samples reflects measures of water availability. Australian Journal of Plant Physiology 26, 185–199.

Heaton, T.H.E., 1999. Spatial, species, and temporal variations in the $^{13}C/^{12}C$ ratios of C_3 plants: implications for palaeodiet studies. Journal of Archaeological Science 26, 637–649.

Hedeen, S., 2008. Big Bone Lick: The Cradle of American Paleontology. University of Kentucky Press, Lexington.

Heusser, L., Maenza-Gmelch, T., Lowell, T., Hinnefeld, R., 2002. Late Wisconsin periglacial environments of the southern margin of the Laurentide Ice Sheet reconstructed from pollen analyses. Journal of Quaternary Science 17, 773–780.

Ives, P.C., Levin, B., Oman, C.L., Rubin, M., 1967. U.S. geological survey radiocarbon dates IX. Radiocarbon 9, 505–529.

Jain, M., Singhvi, A.K., 2001. Limits to depletion of blue-green light stimulated luminescence in feldspars: implications for quartz dating. Radiation Measurements 33, 883–892.

Krasinski, K.E., 2010. Broken Bones and Cutmarks: Taphonomic Analyses and Implications for the Peopling of North America. Ph.D. dissertation. Department of Anthropology, University of Nevada, Reno.

Levin, B., Ives, P.C., Oman, C.L., Rubin, M., 1965. U.S. geological survey radiocarbon dates VIII. Radiocarbon 7, 372–398.

Lewis, R.B., 1996. Kentucky Archaeology. University of Kentucky Press, Lexington.

Liu, Y., Andersen, J.J., Williams, J.W., Jackson, S.T., 2013. Vegetation history in central Kentucky and Tennessee (USA) during the last glacial and deglacial periods. Quaternary Research 79, 189–198.

Metcalfe, J.Z., Longstaffe, F.J., Ballenger, J.A.M., Haynes, C.V.J., 2011. Isotopic paleoecology of Clovis mammoths from Arizona. Proceedings of the National Academy of Sciences 108, 17916–17920.

Metcalfe, J.Z., Longstaffe, F.J., Hodgins, G., 2013. Proboscideans and paleoenvironments of the Pleistocene Great Lakes: landscape, vegetation, and stable isotopes. Quaternary Science Reviews 76, 102–113.

Mortensen, L.A., 2013. The Chronostratigraphy of Big Bone Lick, Kentucky and Its Archaeological Implications. M.A, thesis. Department of Anthropology, University of Cincinnati.

Murray, A.S., Wintle, A.G., 2000. Luminescence dating of quartz using an improved single-aliquot regenerative-dose protocol. Radiation Measurements 32, 57–73.

Murray, A.S., Wintle, A.G., 2003. The single aliquot regenerative dose protocol: potential for improvements in reliability. Radiation Measurements 37, 377–381.

Nadelhoffer, K.J., Fry, B., 1988. Controls on natural Nitrogen-15 and Carbon-13 abundances in forest soil organic matter. Soil Science Society of America Journal 52, 1633–1640. http://dx.doi.org/10.2136/sssaj1988.03615995005200060024x.

Porart, N., 2006. Use of magnetic separation for purifying quartz for luminescence dating. Ancient TL 24, 33–36.

Potter, P.E., 1996. Exploring the Geology of the Cincinnati/Northern Kentucky Region. Kentucky Geological Survey, Lexington.

Ray, L.L., 1974. Geomorphology and Quaternary Geology of the Glaciated Ohio River Valley — A Reconnaissance Study. U. S. Geological Survey Professional Paper 826.

Reimer, P.J., Bard, E., Bayliss, A., Beck, J.W., Blackwell, P.G., Bronk Ramsey, C., Buck, C.E., Edwards, R.L., Friedrich, M., Grootes, P.M., Guilderson, T.P., Haflidason, H., Hajdas, I., Hatté, C., Heaton, T.J., Hoffman, D.L., Hogg, A.G., Hughen, K.A., Kaiser, K.F., Kromer, B., Manning, S.W., Niu, M., Reimer, R.W., Richards, D.A., Scott, M., Southon, J.R., Staff, R.A., Turney, C.S.M., van der Plicht, J., 2013. IntCal13 and Marine13 radiocarbon age calibration curves 0–50,000 years cal BP. Radiocarbon 55, 1869–1887.

Schultz, C.B., Tanner, L.G., Whitmore, F.C., Ray, L.L., Crawford, E.C., 1963. Paleontological investigations at Big Bone Lick State Park, Kentucky: a preliminary report. Science 142 (29), 1167–1169.

Storrs, G.W., Genheimer, R.A., Hedeen, S.E., 2009. In the Footsteps of Lewis and Clark — New Zooarchaeological Excavation at Big Bone Lick, Kentucky. 9th North American Paleontological Convention Abstracts. 3. Cincinnati Museum Center Scientific Contributions, p. 236.

Swadley, W.C., 1969. Geologic Map of the Union Quadrangle, Boone County, Kentucky. United States Geological Survey, Washington D.C.

Tankersley, K.B., 1985. The potential for early man sites at Big Bone Lick, Kentucky. Tennessee Anthropologist 10, 27–49.

Tankersley, K.B., 1986. Bison exploitation by the Fort Ancient peoples of the central Ohio Valley. North American Archaeologist 7, 289–303.

Tankersley, K.B., 1987. Big Bone Lick: A Clovis site in northcentral Kentucky. Current Research in the Pleistocene 4, 36–37.

Tankersley, K.B., 1990. The Paleoindian Period. In: Pollack, D. (Ed.), The Archaeology of Kentucky: Past Accomplishments and Future Directions. Kentucky Heritage Council Press, Frankfort, pp. 75–144.

Tankersley, K.B., 1996. Ice Age Hunters and Gatherers. In: Lewis, R.B. (Ed.), Kentucky Archaeology. University of Kentucky Press, pp. 21–38.

Tankersley, K.B., 2002. In Search of Ice Age Americans. Gibbs Smith Publishers Press, Layton, Utah.

Tankersley, K.B., 2007. Big Bone Lick, Kentucky: Late Pleistocene Archaeology. In: Dalbey, T.S. (Ed.), Geological Aspects of Key Archaeological Sites in Northern Kentucky and Southern Ohio. Ohio Geological Survey, Columbus, pp. 46–50.

Tankersley, K.B., 2009. Late Pleistocene Paleontology and Archaeology of Big Bone Lick, Kentucky. In: Brett, Carl (Ed.), North American Paleontological Convention Field Trip Guide, pp. 95–124.

Tankersley, K.B., Munson, P.J., Tankersley, J.R., 1983. The archaeological geology of the Whitewater–Great Miami–Ohio River Valley. Abstracts with Programs, 96th Annual Meeting 15. Geological Society of America, p. 704.

Tankersley, K.B., Waters, M., Stafford, Y., 2009. Clovis and the American Mastodon at Big Bone Lick, Kentucky. American Antiquity 74, 558–567.

Vogel, J.C., Talma, A.S., Hall-Martin, A.J., Viljoen, P.J., 1990. Carbon and nitrogen isotopes in elephants. South African Journal of Science 86, 147–150.

Widga, C., 2006. Niche variability in late Holocene bison: a perspective from Big Bone Lick, KY. Journal of Archaeological Science 33, 1237–1255.

Wintle, A.G., Murray, A.S., 2006. A review of quartz optically stimulated luminescence characteristics and their relevance in single-aliquot regeneration dating protocols. Radiation Measurements 41, 369–391.